Nonlinear flexural vibration of shear deformable functionally graded spherical shell panel

Vishesh R. Kar [a] and Subrata K. Panda [*]

Department of Mechanical Engineering, National Institute of Technology, Rourkela, India

Abstract.   In this article, nonlinear free vibration behaviour of functionally graded spherical panel is analysed. A nonlinear mathematical model is developed based on higher order shear deformation theory for shallow shell by taking Green-Lagrange type of nonlinear kinematics. The material properties of functionally graded material are assumed to be varying continuously in transverse direction and evaluated using Voigt micromechanical model in conjunction with power-law distribution. The governing equation of the shell panel is obtained using Hamilton's principle and discretised with the help of nonlinear finite element method. The desired responses are evaluated through a direct iterative method. The present model has been validated by comparing the frequency ratio (nonlinear frequency to linear frequency) with those available published literatures. Finally, the effect of geometrical parameters (curvature ratio, thickness ratio, aspect ratio and support condition), power law indices and amplitude of vibration on the frequency ratios of spherical panel have been discussed through numerical experimentations.

Keywords: nonlinear flexural vibration; finite element analysis; FGM; HSDT; Green-Lagrange

1. Introduction

The necessity of advanced materials for aerospace, power, automotive and other engineering fields are focused demanded which can maintain their capabilities even in the extreme environmental conditions. Layered structures have shown their applicability in various weight sensitive industries, but due to residual stresses at the interfaces, de-lamination of layers may occur which causes failure. In functionally graded material (FGM), smooth variation of (metal/ceramic) materials from one surface to another surface results elimination of de-lamination phenomenon. The metals or metal alloys are having good high toughness and strength whereas in the other counterpart, the ceramics have better heat resistance and anti-oxidant properties.

Several studies have already been studied and reported on the analysis and modelling of functionally graded (FG) shell panels based on the different shell theories and the solution techniques (Birman and Byrd 2007, Liew *et al*. 2011, Jha *et al*. 2013, Alijani and Amabili 2014). Talha and Singh (2011) analysed the free vibration of the FG plate in the framework of higher order shear deformation theory (HSDT) by taking Green–Lagrange nonlinearity. Uymaz and

---

∗Corresponding author, Assistant Professor, E-mail: call2subrat@gmail.com; pandask@nitrkl.ac.in
[a] Ph.D. Student, E-mail: visheshkar@gmail.com

Aydogdu (2007) developed 3D solutions for vibration of FG plates under different support conditions using small strain linear elasticity theory. Matsunaga (2008) studied the free vibration and buckling responses of simply-supported FG shallow shell panels by using a 2D higher-order deformation theory. Hosseini-Hashemi *et al*. (2010) computed analytically the free vibration behaviour of moderately thick FG plates for various support conditions. Bich and Nguyen (2012) studied nonlinear vibration of FG cylindrical shell subjected to axial and transverse mechanical loads using displacement method and improved Donnell shell theory. Malekzadeh and Heydarpour (2012) investigated free vibration behaviour of temperature dependent FG cylindrical shells based on the first order shear deformation theory (FSDT). Rahimi *et al*. (2011) investigated the vibration responses of FG cylindrical shells with intermediate ring supports based on Sanders' thin shell theory. Santos *et al*. (2009) proposed a semi-analytical axisymmetric finite element model to investigate the free vibration behaviour of FG cylindrical shell using the 3D linear elastic theory. Haddadpour *et al*. (2007) presented free vibration behaviour of FG cylindrical shell for four different in-plane boundary conditions for different thermal conditions. Patel *et al*. (2005) investigated free vibration characteristics of FG cylindrical shell with elliptical base using higher-order through the thickness approximations based on finite element formulation. Pradyumna and Bandyopadhyay (2008) studied free vibration responses of FG curved panels using HSDT kinematic model and Sanders' shallow shell theory. Pradyumna *et al*. (2010) examined the nonlinear transient vibrations of FG doubly curved panels based on higher-order finite element formulation using New-mark method. Alijani *et al*. (2011a) employed Donnell's nonlinear shallow-shell theory to examine the nonlinear forced vibrations of simply-supported FG doubly curved shallow shells. The authors (Alijani *et al*. 2011b) also investigated the nonlinear forced vibrations of FG curved shells through multi-modal energy approach and pseudo-arc-length continuation and collocation scheme under thermal environment. Sundararajan *et al*. (2005) examined the nonlinear vibration behaviour of FG plates under thermal environment based on FSDT using von Karman's assumptions. Shen and Wang (2014) reported the nonlinear vibration behaviour of FG cylindrical shell panel using the HSDT and von Karman nonlinearity under temperature field. Chorfi and Houmat (2010) approached the harmonic balance method to investigate the nonlinear vibration responses of clamped FG doubly curved shallow shells. Tornabene and Viola (2009) employed the Generalized Differential Quadrature method to obtain the free vibration of FG panels and shells of revolution based on the FSDT.

Based on the review, we note that no study has been reported on the free vibration behaviour of FG spherical shell panel using HSDT mid-plane kinematics with Green-Lagrange nonlinearity. In addition to the above, the present study included all the nonlinear higher order strain terms in the mathematical model to predict the exact responses under severe nonlinearity. Here in this study, the effective material properties of in-homogenous FG shell panel are evaluated using micromechanical model (Gibson *et al*. 1995) in conjunction with power-law distribution to achieve the smooth gradation between different constituents. Hence, an attempt has been made first time to solve such complex problem numerically for FG shell panel and to develop better understanding in small strain and large translation/rotation regime. The governing equation of vibrated FG shell panel is derived using Hamilton's principle for the developed mathematical model. The model has been discretised via suitable finite element steps and the desired responses are obtained using a direct iterative method. The convergence test of the present developed model has been carried out to stabilise the presently proposed model. Subsequently, few comparisons have been made for both linear and nonlinear cases to exhibit the efficacy and necessity of the present developed model. Finally, the influence of different parameters such as power-law index,

thickness ratios, aspect ratios, curvature ratios, amplitude ratios and support constraints on frequency ratios (nonlinear frequency to linear frequency) are studied in details.

2. Mathematical formulations

In the present analysis, a spherical FG shell panel is considered with uniform thickness '*h*' and sides *a* and *b* as shown in Fig. 1. Here, R_x and R_y are the principal radii of curvatures of the shell panel along *x* and *y* directions, respectively. The principal radii of curvature of spherical panel is assumed as, $R_x = R_y = R$.

2.1 Kinematic model of FG panel

The following HSDT displacement field is used for the FG shell panel to derive the mathematical model as in Reddy (2003).

$$\left.\begin{aligned}
\overline{u}(x,y,z,t) &= u_0(x,y,t) + z\theta_x(x,y,t) + z^2 u_0^*(x,y,t) + z^3\theta_x^*(x,y,t) \\
\overline{v}(x,y,z,t) &= v_0(x,y,t) + z\theta_y(x,y,t) + z^2 v_0^*(x,y,t) + z^3\theta_y^*(x,y,t) \\
\overline{w}(x,y,z,t) &= w_0(x,y,t)
\end{aligned}\right\} \tag{1}$$

where, $\overline{u}, \overline{v}$, and $\overline{w}$ denote the displacements of any point in the given panel along the (*x*, *y*, *z*) coordinates. u_0, v_0 and w_0 are the corresponding mid-plane displacements. θ_x and θ_y are the rotations of transverse normal about the *y* and *x*-axis, respectively. The functions u_0^*, v_0^*, θ_x^* and θ_y^* are the higher order terms in the Taylor series expansion defined in the mid-plane of the shell.

Eq. (1) can also be represented in the matrix form as
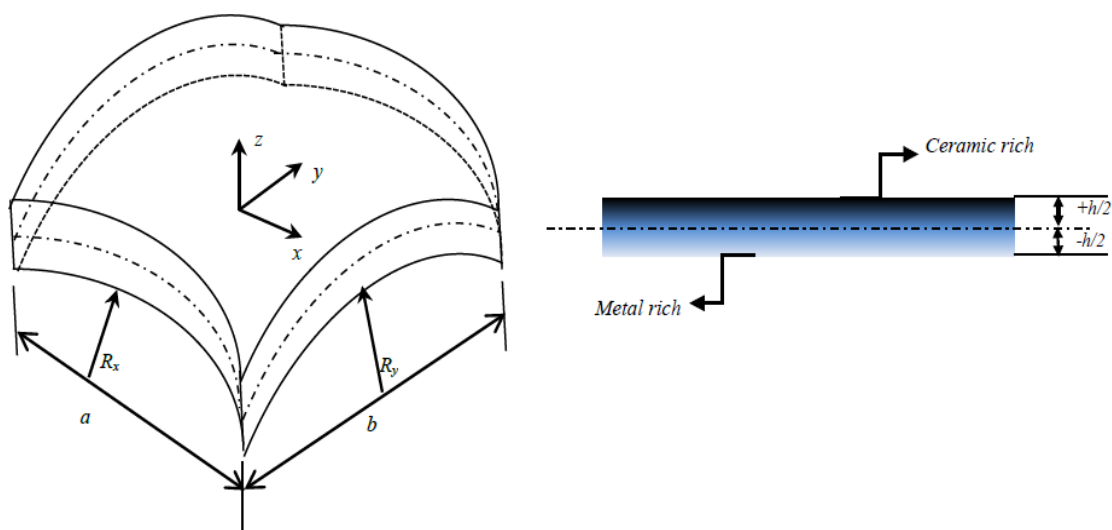
$$\{\delta\} = [f]\{\delta_0\} \tag{2}$$

Fig. 1 Geometry and dimension of spherical FG shell panel

where, $\{\delta\} = \{\bar{u}\ \bar{v}\ \bar{w}\}^T$, $\{\delta_0\} = \{u_0\ v_0\ w_0\ \theta_x\ \theta_y\ u_0^*\ v_0^*\ \theta_x^*\ \theta_y^*\}$, and $[f]$ is the function of thickness coordinate.

2.2 Strain displacement relations

The total strain vector $\{\varepsilon\}$, comprised of linear $\{\varepsilon_L\}$ and nonlinear $\{\varepsilon_{NL}\}$ strains, are defined in Green-Lagrange sense of any material continuum as in (Panda and Singh 2009).

$$\{\varepsilon\} = \begin{Bmatrix} \varepsilon_{xx} \\ \varepsilon_{yy} \\ \gamma_{xy} \\ \gamma_{xz} \\ \gamma_{yz} \end{Bmatrix} = \{\varepsilon_L\} + \{\varepsilon_{NL}\} = \begin{Bmatrix} \bar{u}_{,x} \\ \bar{v}_{,x} \\ \bar{u}_{,y} + \bar{v}_{,x} \\ \bar{u}_{,z} + \bar{w}_{,x} \\ \bar{v}_{,z} + \bar{w}_{,y} \end{Bmatrix} + \begin{Bmatrix} \frac{1}{2}\left[(\bar{u}_{,x})^2 + (\bar{v}_{,x})^2 + (\bar{w}_{,x})^2\right] \\ \frac{1}{2}\left[(\bar{u}_{,y})^2 + (\bar{v}_{,y})^2 + (\bar{w}_{,y})^2\right] \\ (\bar{u}_{,x})(\bar{u}_{,y}) + (\bar{v}_{,x})(\bar{v}_{,y}) + (\bar{w}_{,x})(\bar{w}_{,y}) \\ (\bar{u}_{,z})(\bar{u}_{,x}) + (\bar{v}_{,z})(\bar{v}_{,x}) + (\bar{w}_{,z})(\bar{w}_{,x}) \\ (\bar{u}_{,z})(\bar{u}_{,y}) + (\bar{v}_{,z})(\bar{v}_{,y}) + (\bar{w}_{,z})(\bar{w}_{,y}) \end{Bmatrix} \tag{3}$$

By substituting Eq. (1) in Eq. (3), the strain displacement relation for FG shell panel can be represented in terms of mid-plane strain vectors as

$$\{\varepsilon\} = \begin{Bmatrix} \varepsilon_x^0 \\ \varepsilon_y^0 \\ \varepsilon_{xy}^0 \\ \varepsilon_{xz}^0 \\ \varepsilon_{yz}^0 \end{Bmatrix} + \begin{Bmatrix} \varepsilon_x^4 \\ \varepsilon_y^4 \\ \varepsilon_{xy}^4 \\ \varepsilon_{xz}^4 \\ \varepsilon_{yz}^4 \end{Bmatrix} + z\left[\begin{Bmatrix} k_x^1 \\ k_y^1 \\ k_{xy}^1 \\ k_{xz}^1 \\ k_{yz}^1 \end{Bmatrix} + \begin{Bmatrix} k_x^5 \\ k_y^5 \\ k_{xy}^5 \\ k_{xz}^5 \\ k_{yz}^5 \end{Bmatrix}\right] + z^2\left[\begin{Bmatrix} k_x^2 \\ k_y^2 \\ k_{xy}^2 \\ k_{xz}^2 \\ k_{yz}^2 \end{Bmatrix} + \begin{Bmatrix} k_x^6 \\ k_y^6 \\ k_{xy}^6 \\ k_{xz}^6 \\ k_{yz}^6 \end{Bmatrix}\right]$$

$$+ z^3\left[\begin{Bmatrix} k_x^3 \\ k_y^3 \\ k_{xy}^3 \\ k_{xz}^3 \\ k_{yz}^3 \end{Bmatrix} + \begin{Bmatrix} k_x^7 \\ k_y^7 \\ k_{xy}^7 \\ k_{xz}^7 \\ k_{yz}^7 \end{Bmatrix}\right] + z^4\begin{Bmatrix} k_x^8 \\ k_y^8 \\ k_{xy}^8 \\ k_{xz}^8 \\ k_{yz}^8 \end{Bmatrix} + z^5\begin{Bmatrix} k_x^9 \\ k_y^9 \\ k_{xy}^9 \\ k_{xz}^9 \\ k_{yz}^9 \end{Bmatrix} + z^6\begin{Bmatrix} k_x^{10} \\ k_y^{10} \\ k_{xy}^{10} \\ k_{xz}^{10} \\ k_{yz}^{10} \end{Bmatrix} \tag{4}$$

where, $\{\bar{\varepsilon}_l\} = \{\varepsilon_x^0\ \varepsilon_y^0\ \varepsilon_{xy}^0\ \varepsilon_{xz}^0\ \varepsilon_{yz}^0\ k_x^1\ k_y^1\ k_{xy}^1\ k_{xz}^1\ k_{yz}^1\ k_x^2\ k_y^2\ k_{xy}^2\ k_{xz}^2\ k_{yz}^2\ k_x^3\ k_y^3\ k_{xy}^3\ k_{xz}^3\ k_{yz}^3\}^T$ and

$\{\bar{\varepsilon}_{nl}\} = \begin{Bmatrix} \varepsilon_x^4\ \varepsilon_y^4\ \varepsilon_{xy}^4\ \varepsilon_{xz}^4\ \varepsilon_{yz}^4\ k_x^5\ k_y^5\ k_{xy}^5\ k_{xz}^5\ k_{yz}^5\ k_x^6\ k_y^6\ k_{xy}^6\ k_{xz}^6\ k_{yz}^6\ k_x^7\ k_y^7\ k_{xy}^7\ k_{xz}^7\ k_{yz}^7 \\ k_x^8\ k_y^8\ k_{xy}^8\ k_{xz}^8\ k_{yz}^8\ k_x^9\ k_y^9\ k_{xy}^9\ k_{xz}^9\ k_{yz}^9\ k_x^{10}\ k_y^{10}\ k_{xy}^{10}\ k_{xz}^{10}\ k_{yz}^{10} \end{Bmatrix}^T$ are the

linear and nonlinear mid-plane strain vectors, defined in Appendix A(1).

The above Eq. (3) can also be rearranged in the terms of linear $[T^l]$ and nonlinear $[T^{nl}]$ thickness coordinate matrices, as

$$\{\varepsilon\} = [T^l]\{\bar{\varepsilon}_l\} + [T^{nl}]\{\bar{\varepsilon}_{nl}\} \tag{5}$$

2.3 Finite element formulation

The present FG shell panel is discretised using a nine noded isoparametric quadrilateral Lagrangian element with 81 degrees of freedom per element. Therefore, for any element, the mid-plane displacement vector can be expressed as

$$\{\delta_0\} = \sum_{i=1}^{i=9} [N]\{\delta_{0_i}\} \tag{6}$$

where, $\{\delta_{0_i}\} = \{u_{0_i} \ v_{0_i} \ w_{0_i} \ \theta_{x_i} \ \theta_{y_i} \ u_{0_i}^* \ v_{0_i}^* \ \theta_{x_i}^* \ \theta_{y_i}^*\}^T$ is the ith nodal mid-plane displacement vector and $[N]$ is the shape function.

The linear and nonlinear mid-plane strain vector in terms of nodal displacement vector can be written as

$$\{\overline{\varepsilon}_l\} = [N]\{\delta_{0_i}\}, \{\overline{\varepsilon}_{nl}\} = [A][G]\{\delta_{0_i}\} \tag{7}$$

where, $[B]$ is the product form of differential operators and the shape functions in the linear strain terms. $[A]$ is t function of displacements and $[G]$ is the product form of differential operator and shape functions in the nonlinear strain terms. The individual terms of $[B]$, $[A]$ and $[G]$ matrices are defined in Appendix A(2), A(3) and he A(4), respectively.

2.4 Effective material properties of FGM

In this study, it is assumed that FGMs are varying smoothly along the thickness direction of
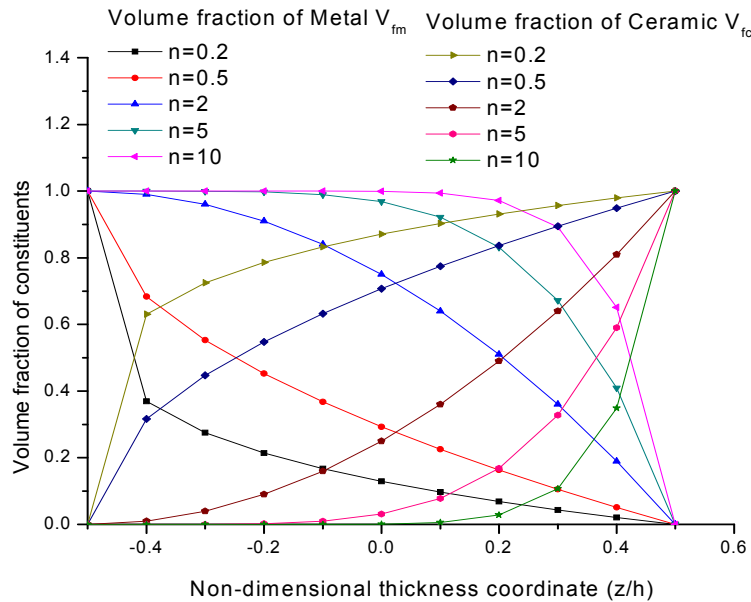

Fig. 2 Variations of volume fractions of FGM constituents (metal and ceramic) along with the non-dimensional thickness coordinate

shell panel from the bottom surface (metal rich) to the top surface (ceramic rich) based on power-law distribution. The effective material property of FGM is evaluated through the Voigt micromechanical model and represented as (Gibson *et al*. 1995)

$$P = (P_t - P_b)V_{f_t} + P_b \tag{8}$$

where, P_b and P_t are the metal and ceramic material properties. V_{fi} is the volume fraction of ceramic material which can be presented according to power-law distribution as (Shen 2009)

$$V_{f_t} = \left(\frac{z}{h} + \frac{1}{2}\right)^n \tag{9}$$

where, n ($0 \le n \le \infty$) is the power-law index which describes the material profile along with the thickness of the FG shell panel. Different material profiles can be generated by varying the power-law index with respect to the ceramic and the metal volume fractions along with the non-dimensional thickness coordinate ($Z = z / h$) as shown in Fig. 2.

2.5 Constitutive relations

The stress strain relationship for FG shell panel can be expressed as

$$\{\sigma\} = \begin{Bmatrix} \sigma_{xx} \\ \sigma_{yy} \\ \tau_{xy} \\ \tau_{xz} \\ \tau_{yz} \end{Bmatrix} = \begin{bmatrix} Q_{11} & Q_{12} & 0 & 0 & 0 \\ Q_{21} & Q_{22} & 0 & 0 & 0 \\ 0 & 0 & Q_{66} & 0 & 0 \\ 0 & 0 & 0 & Q_{55} & 0 \\ 0 & 0 & 0 & 0 & Q_{44} \end{bmatrix} \begin{Bmatrix} \varepsilon_{xx} \\ \varepsilon_{yy} \\ \gamma_{xy} \\ \gamma_{xz} \\ \gamma_{yz} \end{Bmatrix} = [Q]\{\varepsilon\} \tag{10}$$

where, $Q_{11} = Q_{22} = E / (1 - \upsilon^2)$, $Q_{12} = Q_{21} = E * \upsilon / (1 - \upsilon^2)$, $Q_{66} = Q_{55} = Q_{44} = E / 2 * (1 + \upsilon)$.

The strain energy of the curved shell panel can be expressed as

$$U = \frac{1}{2}\int_v \{\varepsilon\}^T \{\sigma\} dV \tag{11}$$

Eq. (11) can be rearranged by substituting strain and stress terms from Eqs. (5) and (10) as

$$U = \frac{1}{2}\int_A \left(\{\bar{\varepsilon}_l\}^T [D_1]\{\bar{\varepsilon}_l\} + \{\bar{\varepsilon}_l\}^T [D_2]\{\bar{\varepsilon}_{nl}\} + \{\bar{\varepsilon}_{nl}\}^T [D_3]\{\bar{\varepsilon}_l\} + \{\bar{\varepsilon}_{nl}\}^T [D_4]\{\bar{\varepsilon}_{nl}\}\right) dA \tag{12}$$

where, $[D_1] = \int_{-h/2}^{+h/2}[T^l]^T [Q][T^l]dz$, $[D_2] = \int_{-h/2}^{+h/2}[T^l]^T [Q][T^{nl}]dz$, $[D_3] = \int_{-h/2}^{+h/2}[T^{nl}]^T [Q][T^l]dz$ and $[D_4] = \int_{-h/2}^{+h/2}[T^{nl}]^T [Q][T^{nl}]dz$.

The kinetic energy of the vibrated FG shell panel is given by

$$T = \frac{1}{2}\int_V \rho\{\dot{\delta}\}^T\{\dot{\delta}\}dV \tag{13}$$

where, ρ is the mass density and $\{\dot{\delta}\}$ is the first order differential of global displacement vector with respect to time.

By substituting Eq. (2) in Eq. (13), the kinetic energy of the FG shell panel for thickness h can be written as

$$T = \frac{1}{2}\int_V \left(\int_{-h/2}^{+h/2}\{\dot{\delta}\}^T[f]^T\rho[f]\{\dot{\delta}_0\}dz \right)dA = \frac{1}{2}\int_A \{\dot{\delta}_0\}^T[m]\{\dot{\delta}_0\}dA \tag{14}$$

where, $[m] = \int_{-h/2}^{+h/2}[f]^T\rho[f]dz$ is the elemental inertia matrix.

2.6 Governing equations

The governing equation of vibrating FG shell panel is obtained by using Hamilton's principle.

$$\delta\int_{t_1}^{t_2}Ldt = 0 \tag{15}$$

where, $L = T - U$.

Now, the final form of the eigenvalue equation is derived using the Eqs. (11)-(15) and rewritten as follows

$$\{[K] - \omega^2[M]\}\{\delta\} = 0 \tag{16}$$

where, $[M]$ is the global mass matrix, ω is the natural frequency of the system and $[K]$ is the global stiffness matrix which includes all the linear and the nonlinear stiffness matrices, $[K_1^l], [K_1^{nl}], [K_2^{nl}]$ and $[K_3^{nl}]$. The linear and nonlinear responses of vibrated FG spherical panel are evaluated by using direct iterative method. The implementation of the iterative method has been discussed as point wise.

(1) As a first step, the elemental stiffness and mass matrices are computed.
(2) These elemental matrices are assembled to give global stiffness and mass matrices.
(3) To obtain the linear response of FG panel, linear eigenvalue equation is solved by setting other nonlinear stiffness matrices equal to zero.
(4) The corresponding eigenvector is extracted through an eigenvector extraction algorithm and normalized and scaled up using amplitude ratio (W_{max} / h, where, W_{max} is the maximum central deflection and h is thickness of the panel) for finding nonlinear stiffness matrices and updating the same, successively.
(5) The above step will be continued until the nonlinear frequency parameter evaluated from the two successive iterations are reached the tolerance limit ($\leq 10^{-3}$).

3. Results and discussions

The desired responses of FG spherical panel are obtained using a nonlinear finite element code developed in MATLAB environment based on the proposed and developed nonlinear mathematical model. The material properties of FGM constituents are assumed to be temperature-independent for the present analysis and presented in Table 1. The support conditions (clamped C, simply-supported S and hinged H) are employed to avoid rigid body motion as well as to reduce the number of constraints. The details of different support conditions are discussed in detail in Table 2. The proposed and developed model has been validated by comparing the results with those available published literatures. Subsequently, the influences of parameters (the power-law indices (n), the thickness ratios (a / h), the curvature ratios (R / a), the aspect ratio (a / b), the amplitude ratios (W_{max} / h) and the support conditions) on the free vibration responses of FG spherical panel are obtained by solving sets of numerical experimentations and discussed.

3.1 Convergence and comparison study

As a first step, the convergence behaviour of the numerical responses has been obtained and shown in Fig. 3. The figure shows, non-dimensional fundamental frequency parameter $\left(\overline{\omega} = \omega ab / h\sqrt{(12(1 - v_m^2)\rho_m / E_m)}\right)$ with the mesh refinement of a simply-supported square FG ($Al /$ ZrO_2) spherical panel. The responses are plotted for three different power-law indices ($n = 0.5, 2$ and 10), $R / a = 50$ and $a / h = 100$. It can be easily seen that the responses are converging well with the mesh refinement and a (6×6) mesh is sufficient enough to compute the desired responses.

Now, the linear frequency responses are obtained using the proposed and developed model for a simply-supported FG (Al / Al_2O_3) spherical panel and compared with Matsunaga (2008) for different parameters i.e., two curvature ratios and six power-law indices and presented in Table 3. It is clear from the table that the responses obtained using present numerical model is in well agreement with the 2D exact solution (Matsunaga 2008) for various parameters as discussed earlier. In continuation to the linear case, one more comparison study has been made to exhibit the nonlinear behaviour of vibrated FG panel and the details are discussed in the subsequent paragraph.

In this section, the convergence and comparison studies of nonlinear behaviour have been examined for a flat panel case. For the computational purpose, a simply-supported square FG ($SUS304 / Si_3N_4$) flat panel ($a / h = 10$, $n = 2$) is being analysed and the responses are plotted in Fig. 4. It is clearly observed that, the values are converging well with mesh refinement and a (6×6) mesh is sufficient to obtain the further results. The present results are also showing good agreement with Sundararajan *et al.* (2005) for different amplitude ratios. It is interesting to note that, the present frequency ratios are comparatively lower than the reference for each amplitude ratios. It is because of the fact that the present model is being developed based on Green-Lagrange nonlinearity in the framework of the HSDT whereas the reference is based on the FSDT with von-Karman nonlinearity. In addition to that, the present model has been formulated by taking the effect of all the nonlinear higher order terms which makes the panel more flexible as compared to the reference. It is also worthy to mention that the von-Karman nonlinearity is unable to count both large rotation and translation terms when the structure exposed to sever nonlinearity and this in turn makes the model inadequate to predict the desired responses.

3.2 Numerical examples

In order to check the robustness of the present mathematical model of shear deformable FG shallow shell model, some numerical examples have been analysed and discussed for different

parameters. In this section, aluminum and zirconia are considered as metal and ceramic, respectively.

Table 1 Material properties of the FGM constituents

Materials		Properties		
		Young's modulus E (GPa)	Poisson's ratio v	Density ρ (kg/m^3)
Metal	Aluminum (Al)	70	0.3	2707
	Stainless steel ($SUS304$)	207.78	0.28	8166
Ceramic	Zirconia (ZrO_2)	151	0.3	3000
	Silicon nitrate (Si_3N_4)	322.27	0.28	2370
	Alumina (Al_2O_3)	380	0.3	3800

Table 2 Sets of support condition

CCCC	$u_0 = v_0 = w_0 = \theta_x = \theta_y = u_0^* = v_0^* = \theta_x^* = \theta_y^* = $ at $x = 0, a$ and $y = 0, b$
SSSS	$v_0 = w_0 = \theta_y = v_0^* = \theta_y^* = $ at $x = 0, a$; $u_0 = w_0 = \theta_x = u_0^* = \theta_x^* = $ at $y = 0, b$
SCSC	$v_0 = w_0 = \theta_y = v_0^* = \theta_y^* = $ at $x = 0, a$; $u_0 = v_0 = w_0 = \theta_x = \theta_y = u_0^* = v_0^* = \theta_x^* = \theta_y^* = $ at $y = 0, b$
HHHH	$u_0 = v_0 = w_0 = \theta_y = v_0^* = \theta_y^* = $ at $x = 0, a$; $u_0 = v_0 = w_0 = \theta_x = u_0^* = \theta_x^* = 0$ at $y = 0, b$

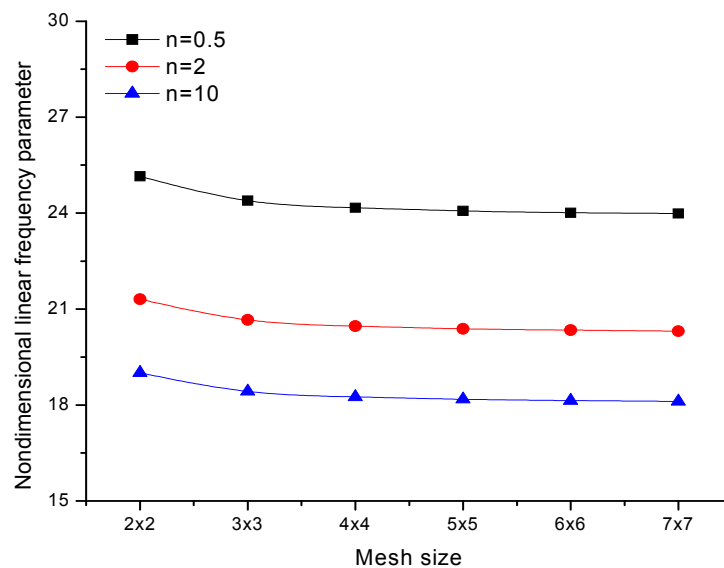

Fig. 3 Non-dimensional linear frequency parameter of a simply-supported square FG (Al/ZrO$_2$) spherical panel ($R / a = 50$, $a / h = 100$) for different mesh size

Table 3 Comparison of linear frequency parameter ($\overline{\omega} = \omega h \sqrt{\rho_c / E_c}$) for a simply-supported FG (Al / Al_2O_3) spherical panel ($a / b = 1$, $a / h = 10$)

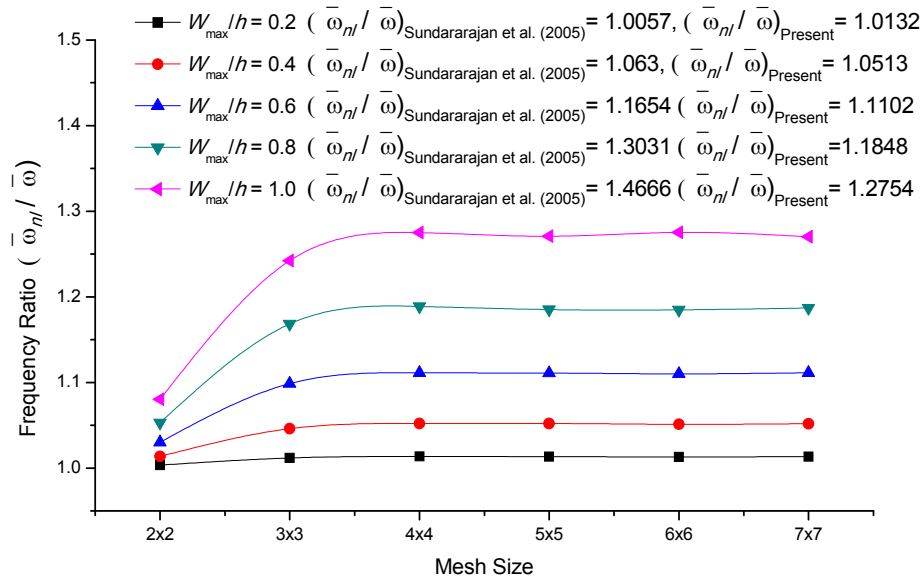| R / a	n	0	0.5	1	4	10	∞
1	Present	0.1078	0.0834	0.0719	0.0526	0.0457	0.0381
	Matsunaga(2008)	0.09782	0.09782	0.09047	0.07453	0.06677	0.05577
2	Present	0.0744	0.0568	0.0486	0.0364	0.0324	0.0263
	Matsunaga(2008)	0.07514	0.06569	0.06006	0.05034	0.04643	0.03826

Fig. 4 Convergence and comparison of frequency ratios of a simply-supported square FG (*SUS304* / *Si₃N₄*) flat panel ($a / h = 10$, $n = 2$) for different amplitude ratios
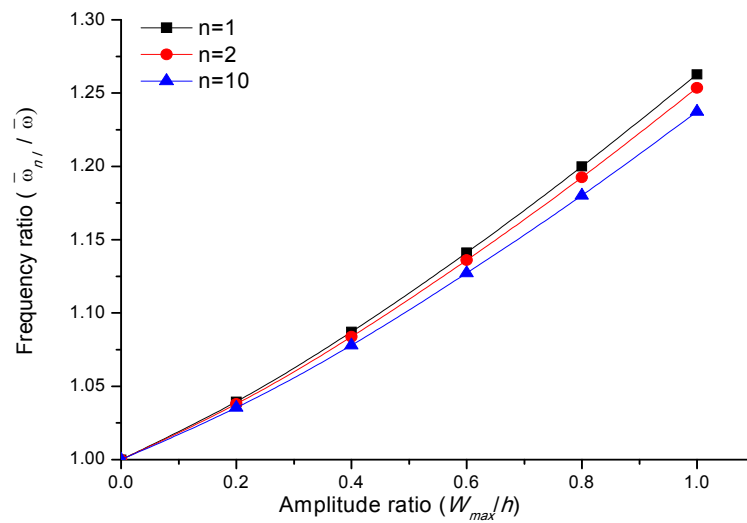

Fig. 5 Influence of power-law index on frequency ratio of simply-supported square FG spherical panel
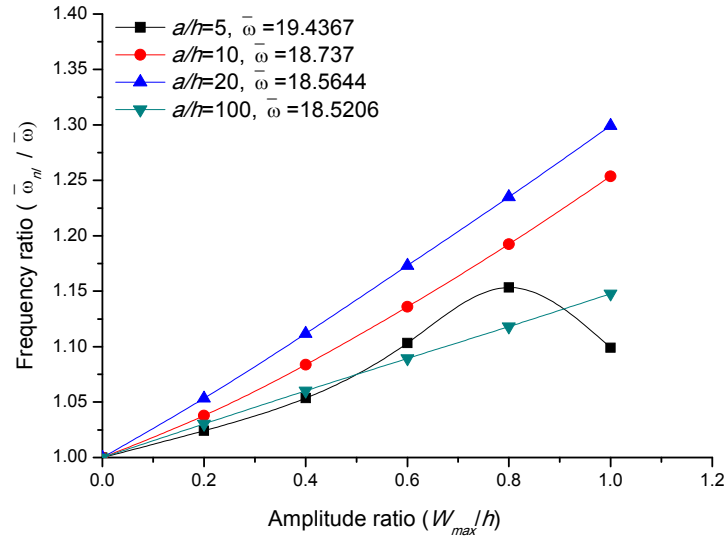
Fig. 6 Influence of thickness ratio on frequency ratio of simply-supported square FG spherical panel

Fig. 5 shows the frequency ratio of a simply-supported square FG (Al/ZrO_2) spherical panel ($R/a = 5$, $a/h = 10$) for different amplitude ratios and power-law indices ($n = 0.5, 2, 10$). It is observed that the frequency ratio decreases with increase in power-law indices that means the nonlinearity is higher for ceramic rich phase (high stiffness) and lower for metal rich phase (low stiffness).

Fig. 6 shows the effect of thickness ratios on the frequency ratios of a square simply-supported FG (Al/ZrO_2) spherical shell panel ($R/a = 5$, $n = 2$) for different amplitude ratios. It is interesting to observe that, as the thickness ratio increases from 5 to 20, the frequency ratios increase for each
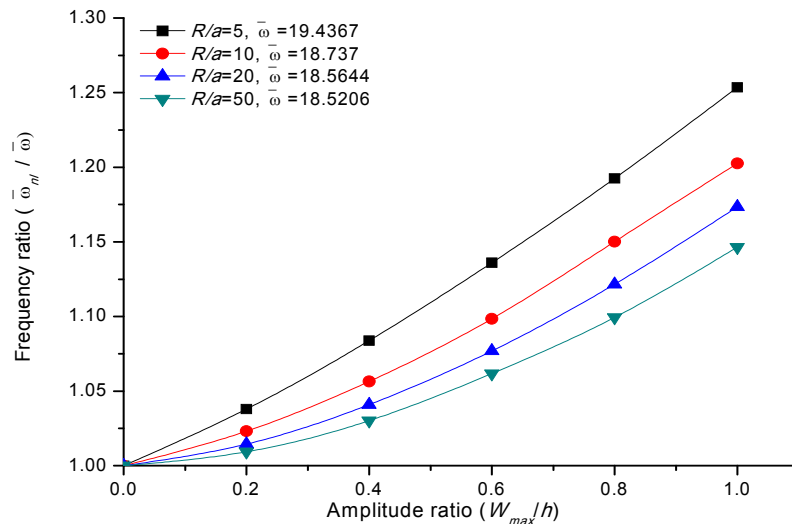

Fig. 7 Influence of curvature ratio on frequency ratio of simply-supported square FG (Al/ZrO_2)
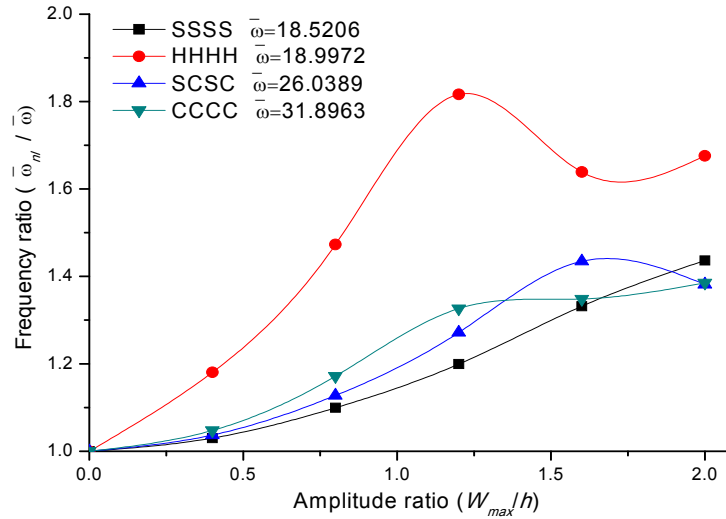spherical ($a/h = 10$) panel ($n = 2$)

Fig. 8 Influence of support condition on frequency ratio of square FG (Al/ZrO_2) spherical panel
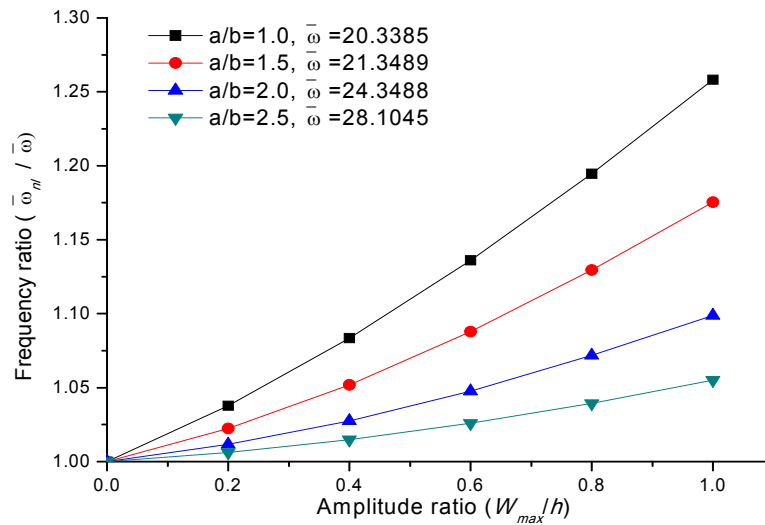

Fig. 9 Influence of aspect ratio on frequency ratio of simply-supported FG spherical panel

amplitude ratios. It is also noted that the frequency ratios are decreasing at $a/h = 100$. This is because of the fact the responses in small strain and large rotation and/or translational problem may not follow a monotonous behaviour.

Fig. 7 shows the effect of curvature ratios on the frequency ratios of a simply-supported square FG (Al/ZrO_2) spherical panel ($n = 2$, $a/h = 10$). It is observed that the frequency ratio decreases with the increase in curvature ratios because as the curvature ratio increases the panel becomes flat. It is also well known that the shell structures have higher membrane stiffness as compared to the flat panel and the amplitude of vibration have less effect on the curved panel in comparison to flat panel.

Fig. 8 presents the frequency ratios of a square FG (Al/ZrO_2) spherical panel ($n=2$, $a/h = 100$, $R/a = 50$) for different types of support conditions and amplitude ratios. It is observed that the responses are following the expected line for every linear case whereas the nonlinearity effect is predominant for hinged support (HHHH). It can also be observed that the frequency ratio increases smoothly up to $W_{max}/h = 1.2$ for each case and it suddenly drops for higher amplitude. This type of non-repetitive behaviour can only be observed by taking full nonlinearity in geometry as in the present case.

Fig. 9 shows the variation of frequency ratios of a simply-supported FG (Al/ZrO_2) spherical panel ($n=2$, $a/h = 100$, $R/a = 50$) for different aspect ratios at different amplitude ratios. It can be observed that the frequency ratio decreases with increase in aspect ratios for all the values of amplitude ratios. This is true that aspect ratio has a considerable effect on stiffness matrix and as the aspect ratio increases the panel loses its geometry from square. In addition to that, nonlinear vibration is not only the functions of linear stiffness and mass matrix but also depending upon nonlinear stiffness matrix and their corresponding amplitude ratios. Hence, the effects can be observed for better understanding.

4. Conclusions

The nonlinear free vibration behaviour of FG spherical shell panel are analysed based on the HSDT mid-plane kinematics (nine degree-of-freedom per node) by taking the geometric nonlinearity in Green-Lagrange sense. The FGM properties are taken as the function of thickness coordinate based on power-law distribution of the volume fractions and invariant with the temperature. Finally, to achieve the true flexure of the panel all the nonlinear higher order terms are taken in the present formulation. Finite element steps are employed by using a nine node isoparametric Lagrangian element to obtain the elemental equations. The governing equations of vibrated FG panel have been obtained using Hamilton's principle and solved using direct iterative method. The accuracy of the developed nonlinear model has been shown through the convergence and comparison. In order to demonstrate the influences of different material and geometrical parameters have been illustrated by solving some new examples. It is observed that, the frequency ratios are increasing with increase in amplitude ratios and thickness ratios whereas decreasing with increase in power law indices, curvature ratios and aspect ratios.

References

Alijani, F. and Amabili, M. (2014), "Non-linear vibrations of shells: A literature review from 2003 to 2013", *Int. J. Nonlinear Mech.*, **58**, 233-257.

Alijani, F., Amabili, M., Karagiozis, K. and Bakhtiari-Nejad, F. (2011a), "Nonlinear vibrations of functionally graded doubly curved shallow shells", *J. Sound Vib.*, **330**(7), 1432-1454.

Alijani, F., Amabili, M., Karagiozis, K. and Bakhtiari-Nejad, F. (2011b), "Thermal effects on nonlinear vibrations of functionally graded doubly curved", *Compos. Struct.*, **93**(10), 2541-2553.

Bich, D.H. and Nguyen, N.X. (2012), "Nonlinear vibration of functionally graded circular cylindrical shells based on improved Donnell equations", *J. Sound Vib.*, **331**(25), 5488-5501.

Birman, V. and Byrd, L.W. (2007), "Modeling and analysis of functionally graded materials and structures", *Appl. Mech. Rev.*, **60**(5), 195-216.

Chorfi, S.M. and Houmat, A. (2010), "Non-linear free vibration of a functionally graded doubly-curved shallow shell of elliptical plan-form", *Compos. Struct.*, **92**(10), 2573-2581.

Gibson, L.J., Ashby, M.F., Karam, G.N., Wegst, U. and Shercliff, H.R. (1995), "Mechanical properties of natural materials. II. Microstructures for mechanical efficiency", *Proc. R. Soc. A*, **450**(1938), 141-162.

Haddadpour, H., Mahmoudkhani, S. and Navazi, H.M. (2007), "Free vibration analysis of functionally graded cylindrical shells including thermal effects", *Thin-Wall. Struct.*, **45**(6), 591-599.

Hosseini-Hashemi, Sh., Taher, H.R.D., Akhavan, H. and Omidi, M. (2010), "Free vibration of functionally graded rectangular plates using first-order shear deformation plate theory", *Appl. Math. Model.*, **34**(5), 1276-1291.

Jha, D.K., Kant, T. and Singh, R.K. (2013), "A critical review of recent research on functionally graded plates", *Compos. Struct.*, **96**, 833-849.

Liew, K.M., Zhao, X. and Ferreira, A.J.M. (2011), "A review of meshless methods for laminated and functionally graded plates and shells", *Compos. Struct.*, **93**(8), 2031-2041.

Malekzadeh, P. and Heydarpour, Y. (2012), "Free vibration analysis of rotating functionally graded cylindrical shells in thermal environment", *Compos. Struct.*, **94**(9), 2971-2981.

Matsunaga, H. (2008), "Free vibration and stability of functionally graded shallow shells according to a 2D higher-order deformation theory", *Compos. Struct.*, **84**(2),132-146.

Panda, S.K. and Singh, B.N. (2009), "Nonlinear free vibration of spherical shell panel using higher order shear deformation theory – A finite element approach", *Int. J. Pres. Ves. Pip.*, **86**(6), 373-383.

Patel, B.P., Gupta, S.S., Loknath, M.S. and Kadu, C.P. (2005), "Free vibration analysis of functionally graded elliptical cylindrical shells using higher-order theory", *Compos. Struct.*, **69**(3), 259-270.

Pradyumna, S. and Bandyopadhyay, J.N. (2008), "Free vibration analysis of functionally graded curved panels using a higher-order finite element formulation", *J. Sound Vib.*, **318**(1-2), 176-192.

Pradyumna, S., Nanda, N. and Bandyopadhyay, J.N. (2010), "Geometrically nonlinear transient analysis of functionally graded shell panels using a higher-order finite element formulation", *J. Mech. Engg. Res.*, **2**(2), 39-51.

Rahimi, G.H., Ansari, R. and Hemmatnezhad, M. (2011), "Vibration of functionally graded cylindrical shells with ring support", *Sci. Iran. Trans. B*, **18**(6), 1313-1320.

Reddy, J.N. (2003), *Mechanics of Llaminated Composite: Plates and Shells-Theory and Analysis*, (2nd Edition), CRC press, Boca Raton, FL, USA.

Santos, H., Soares, C.M.M., Soares, C.A.M. and Reddy, J.N. (2009), "A semi-analytical finite element model for the analysis of cylindrical shells made of functionally graded materials", *Compos. Struct.*, **91**(4), 427-432.

Shen, H.S. (2009), *Functionally Graded Material: Nonlinear Analysis of Plates & Shells*, CRC press, Boca Raton, FL, USA.

Shen, H.S. and Wang, H. (2014), "Nonlinear vibration of shear deformable FGM cylindrical panels resting on elastic foundations in thermal environments", *Compos. Part B-Eng.*, **60**, 167-177.

Sundararajan, N., Prakash, T. and Ganapathi, M. (2005), "Nonlinear free flexural vibrations of functionally graded rectangular and skew plates under thermal environments", *Finite Elem. Anal. Des.*, **42**(2), 152-168.

Talha, M. and Singh, B.N. (2011), "Large amplitude free flexural vibration analysis of shear deformable FGM plates using nonlinear finite element method", *Finite Elem. Anal. Des.*, **47**(4), 394-401.

Tornabene, F. and Viola, E. (2009), "Free vibration analysis of functionally graded panels and shells of revolution", *Meccanica*, **44**(3), 255-281.

Uymaz, B. and Aydogdu, M. (2007), "Three-dimensional vibration analysis of functionally graded plates under various boundary conditions", *J. Reinf. Plast. Comp.*, **26**(18), 1847-1863.

BU

Appendix A

Linear mid-plane strain terms

$$\varepsilon_x^0 = u_{,x}, \qquad \varepsilon_y^0 = v_{,y}, \qquad \varepsilon_{xy}^0 = u_{,y} + v_{,x}, \qquad \varepsilon_{xz}^0 = w_{,x} + \theta_x, \qquad \varepsilon_{yz}^0 = w_{,y} + \theta_y,$$

$$k_x^1 = \theta_{x,x}, \qquad k_y^1 = \theta_{y,y}, \qquad k_{xy}^1 = \theta_{x,y} + \theta_{y,x}, \qquad k_{xz}^1 = 2u_0^* - \theta_x / R_x, \qquad k_{yz}^1 = 2v_0^* - \theta_y / R_y,$$

$$k_x^2 = u_{0,x}^*, \qquad k_y^2 = v_{0,y}^*, \qquad k_{xy}^2 = u_{0,y}^* + v_{0,x}^*, \qquad k_{xz}^2 = 3\theta_x^* - u_0^* / R_x, \qquad k_{yz}^2 = 3\theta_y^* - v_0^* / R_y,$$

$$k_x^3 = \theta_{x,x}^*, \qquad k_y^3 = \theta_{y,y}^*, \qquad k_{xy}^3 = \theta_{x,y}^* + \theta_{y,x}^*, \qquad k_{xz}^3 = -\theta_x^* / R_x, \qquad k_{yz}^3 = -\theta_y^* / R_y.$$

Nonlinear mid-plane strain terms

$$\varepsilon_x^4 = ?\ u_{,x}^2 + ?\ v_{,x}^2 + ?\ w_{,x}^2, \qquad \varepsilon_y^4 = ?\ u_{,y}^2 + ?\ v_{,y}^2 + ?\ w_{,y}^2$$

$$\varepsilon_{xy}^4 = u_{,x}u_{,y} + v_{,x}v_{,y} + w_{,x}w_{,y}, \qquad \varepsilon_{xz}^4 = u_{,x}\theta_x + v_{,x}\theta_y, \qquad \varepsilon_{yz}^4 = u_{,y}\theta_x + v_{,y}\theta_y$$

$$k_x^5 = u_{,x}\theta_{x,x} + v_{,x}\theta_{y,x} - w_{,x}\theta_x / R_x, \qquad k_y^5 = u_{,x}\theta_{x,y} + v_{,y}\theta_{y,y} - w_{,y}\theta_y / R_y,$$

$$k_{xy}^5 = u_{,x}\theta_{x,y} + u_{,y}\theta_{x,x} + v_{,x}\theta_{y,y} + v_{,y}\theta_{y,x} - w_{,x}\theta_y / R_y - w_{,y}\theta_x / R_x,$$

$$k_{xz}^5 = 2u_{,x}u_0^* + 2v_{,x}v_0^* + \theta_{,x}\theta_x + \theta_{y,x}\theta_y,$$

$$k_{yz}^5 = 2u_{,y}u_0^* + 2v_{,y}v_0^* + \theta_{,x}\theta_x + \theta_{y,y}\theta_y,$$

$$k_x^6 = u_{,x}u_{0,x}^* + v_{,x}v_{0,x}^* - w_{,x}u_0^* / R_x + \tfrac{1}{2}\theta_{x,x}^2 + \tfrac{1}{2}\theta_{y,x}^2 + \tfrac{1}{2}\theta_x^2 / R_x^2$$

$$k_y^6 = u_{,y}u_{0,y}^* + v_{,y}v_{0,y}^* - w_{,y}v_0^* / R_y + \tfrac{1}{2}\theta_{x,y}^2 + \tfrac{1}{2}\theta_{y,y}^2 + \tfrac{1}{2}\theta_y^2 / R_y^2,$$

$$k_{xy}^6 = u_{,x}u_{0,y}^* + u_{,y}u_{0,x}^* + v_{,x}v_{0,y}^* + v_{,y}v_{0,x}^* - w_{,x}v_0^* / R_y - w_{,y}u_0^* / R_x + \theta_{x,x}\theta_{x,y} + \theta_{y,x}\theta_{y,y} + \theta_x\theta_y / R_xR_y,$$

$$k_{xz}^6 = 3u_{,x}\theta_x^* + 3v_{,x}\theta_y^* + 2\theta_{x,x}u_0^* + 2\theta_{y,x}v_0^* + u_{0,x}^*\theta_x + v_{0,x}^*\theta_y,$$

$$k_{yz}^6 = 3u_{,y}\theta_x^* + 3v_{,y}\theta_y^* + 2\theta_{x,y}u_0^* + 2\theta_{y,y}v_0^* + u_{0,y}^*\theta_x + v_{0,y}^*\theta_y,$$

$$k_x^7 = u_{,x}\theta_{x,x}^* + v_{,x}\theta_{y,x}^* - w_{,x}\theta_x^* / R_x + \theta_{x,x}u_{0,x}^* + \theta_{y,x}v_{0,x}^* + \theta_x u_0^* / R_x^2,$$

$$k_y^7 = u_{,y}\theta_{x,y}^* + v_{,y}\theta_{y,y}^* - w_{,y}\theta_y^* / R_y + \theta_{x,y}u_{0,y}^* + \theta_{y,y}v_{0,y}^* + \theta_y v_0^* / R_y^2,$$

$$k_{xy}^7 = u_{,x}\theta_{x,y}^* + u_{,y}\theta_{x,x}^* + v_{,x}\theta_{y,y}^* + v_{,y}\theta_{y,x}^* - w_{,x}\theta_y^* / R_y - w_{,y}\theta_x^* / R_x + \theta_{x,x}u_{0,y}^* + \theta_{x,y}u_{0,x}^* + \theta_{y,x}v_{0,y}^*$$
$$+ \theta_{y,y}v_{0,x}^* + \theta_x v_0^* / R_xR_y + \theta_y u_0^* / R_xR_y$$

$$k_{xz}^7 = 3\theta_{x,x}\theta_x^* + 3\theta_{y,x}\theta_y^* + 2u_{0,x}^*u_0^* + 2v_{0,x}^*v_0^* + \theta_{x,x}^*\theta_x + \theta_{y,x}^*\theta_y,$$

$$k_{yz}^7 = 3\theta_{x,y}\theta_x^* + 3\theta_{y,y}\theta_y^* + 2u_{0,y}^*u_0^* + 2v_{0,y}^*v_0^* + \theta_{x,y}^*\theta_x + \theta_{y,y}^*\theta_y,$$

$$k_x^8 = \theta_{x,x}\theta_{x,x}^* + \theta_{y,x}\theta_{y,x}^* + \tfrac{1}{2}\left(u_{0,x}^*\right)^2 + \tfrac{1}{2}\left(v_{0,x}^*\right)^2 + \theta_x\theta_x^* / R_x^2 + \tfrac{1}{2}(u_0^* / R_x)^2,$$

$$k_y^8 = \theta_{x,y}\theta_{x,y}^* + \theta_{y,y}\theta_{y,y}^* + \tfrac{1}{2}\left(u_{0,y}^*\right)^2 + \tfrac{1}{2}\left(v_{0,y}^*\right)^2 + \theta_y\theta_y^* / R_y^2 + \tfrac{1}{2}(v_0^* / R_y)^2,$$

$$k_{xy}^8 = \theta_{x,x}\theta_{x,y}^* + \theta_{x,y}\theta_{x,x}^* + \theta_{y,x}\theta_{y,y}^* + \theta_{y,y}\theta_{y,x}^* + u_{0,x}^*u_{0,y}^* + v_{0,x}^*v_{0,y}^* + \theta_x\theta_y^* / R_xR_y + \theta_y\theta_x^* / R_xR_y + u_0^*v_0^* / R_xR_y,$$

$$k_{xz}^8 = 3u_{0,x}^*\theta_x^* + 3v_{0,x}^*\theta_y^* + 2\theta_{x,x}^*u_0^* + 2\theta_{y,x}^*v_0^*, \qquad\qquad k_{yz}^8 = 3u_{0,y}^*\theta_x^* + 3v_{0,y}^*\theta_y^* + 2\theta_{x,y}^*u_0^* + 2\theta_{y,y}^*v_0^*,$$

$$k_x^9 = u_{0,x}^*\theta_{x,x}^* + v_{0,x}^*\theta_{y,x}^* + u_0^*\theta_x^* / R_x^2, \qquad\qquad k_y^9 = u_{0,y}^*\theta_{x,y}^* + v_{0,y}^*\theta_{y,y}^* + v_0^*\theta_y^* / R_y^2,$$

$$k_{xy}^9 = u_{0,x}^*\theta_{x,y}^* + u_{0,y}^*\theta_{x,x}^* + v_{0,x}^*\theta_{y,y}^* + v_{0,y}^*\theta_{y,x}^* + u_0^*\theta_y^* / R_xR_y + v_0^*\theta_x^* / R_xR_y,$$

$$k_{xz}^9 = 3\theta_{x,x}^*\theta_x^* + 3\theta_{y,x}^*\theta_y^*, \qquad k_{yz}^9 = 3\theta_{x,y}^*\theta_x^* + 3\theta_{y,y}^*\theta_y^*,$$

$k_x^{10} = \frac{1}{2}(\theta_{x,x}^*)^2 + \frac{1}{2}(\theta_{y,x}^*)^2 + \frac{1}{2}(\theta_x^*/R_x)^2$, $\qquad\qquad k_y^{10} = \frac{1}{2}(\theta_{x,y}^*)^2 + \frac{1}{2}(\theta_{y,y}^*)^2 + \frac{1}{2}(\theta_y^*/R_y)^2$,

$k_{xy}^{10} = \theta_{x,x}^*\theta_{x,y}^* + \theta_{y,x}^*\theta_{y,y}^* + \theta_x^*\theta_y^*/R_x R_y$.

where, the expressions of $u_{,x}$, $u_{,y}$, $v_{,x}$, $v_{,y}$, $w_{,x}$ and $w_{,y}$ are

$u_{,x} = \partial u_0 / \partial x + w_0 / R_x$, $\qquad\qquad u_{,y} = \partial u_0 / \partial y + w_0 / R_{xy}$

$v_{,x} = \partial v_0 / \partial x + w_0 / R_{xy}$, $\qquad\qquad v_{,y} = \partial v_0 / \partial y + w_0 / R_y$,

$w_{,x} = \partial w_0 / \partial x - u_0 / R_x$, $\qquad\qquad w_{,y} = \partial w_0 / \partial y - v_0 / R_y$. $\qquad$ A(1)

Individual terms of matrix [B]

$[B]_{1,1} = \partial/\partial x$, $[B]_{1,3} = 1/R_x$, $[B]_{2,2} = \partial/\partial y$, $[B]_{2,3} = 1/R_y$,

$[B]_{3,1} = \partial/\partial y$, $[B]_{3,2} = \partial/\partial x$, $[B]_{3,3} = 2/R_{xy}$, $[B]_{4,1} = -1/R_x$, $[B]_{4,3} = \partial/\partial x$, $[B]_{4,4} = 1$,

$[B]_{5,2} = -1/R_y$, $[B]_{5,3} = \partial/\partial x$, $[B]_{5,5} = 1$, $\qquad$ $[B]_{6,4} = \partial/\partial x$, $[B]_{7,5} = \partial/\partial y$, $[B]_{8,4} = \partial/\partial y$,

$[B]_{8,5} = \partial/\partial x$, $[B]_{9,4} = -1/R_x$, $[B]_{9,6} = 2$, $\qquad$ $[B]_{10,5} = -1/R_y$, $[B]_{10,7} = 2$, $\qquad$ $[B]_{11,6} = \partial/\partial x$,

$[B]_{12,7} = \partial/\partial y$, $[B]_{13,6} = \partial/\partial y$, $[B]_{13,7} = \partial/\partial x$, $[B]_{14,6} = -1/R_x$, $[B]_{14,8} = 2$, $\qquad$ $[B]_{15,7} = -1/R_y$,

$[B]_{15,9} = 2$, $\qquad$ $[B]_{16,8} = \partial/\partial x$, $[B]_{17,9} = \partial/\partial y$, $[B]_{18,8} = \partial/\partial y$, $[B]_{18,9} = \partial/\partial x$,

$[B]_{19,8} = -1/R_x$, $[B]_{20,9} = -1/R_y$. $\qquad$ A(2)

Individual terms of matrix [A]

$[A]_{1,1} = \frac{1}{2}u_{,x}$, $[A]_{1,3} = \frac{1}{2}v_{,x}$, $[A]_{1,5} = \frac{1}{2}w_{,x}$, $[A]_{2,2} = \frac{1}{2}u_{,y}$, $[A]_{2,4} = \frac{1}{2}v_{,y}$, $[A]_{2,6} = \frac{1}{2}w_{,y}$,

$[A]_{3,1} = u_{,y}$, $\qquad$ $[A]_{3,3} = v_{,y}$, $\qquad$ $[A]_{3,5} = w_{,y}$, $[A]_{4,1} = \theta_x$, $\qquad$ $[A]_{4,3} = \theta_y$,

$[A]_{5,2} = \theta_x$, $\qquad$ $[A]_{5,4} = \theta_y$, $\qquad$ $[A]_{6,1} = \theta_{x,x}$, $[A]_{6,3} = \theta_{y,x}$, $[A]_{6,5} = -\theta_x/R_x$,

$[A]_{7,2} = \theta_{x,y}$, $[A]_{7,4} = \theta_{y,y}$, $[A]_{7,6} = -\theta_y/R_y$, $[A]_{8,1} = \theta_{x,y}$, $\qquad$ $[A]_{8,2} = \theta_{x,x}$, $\qquad$ $[A]_{8,3} = \theta_{y,y}$,

$[A]_{8,4} = \theta_{y,x}$, $[A]_{8,5} = -\theta_y/R_y$, $[A]_{8,6} = -\theta_x/R_x$,

$[A]_{9,1} = 2u_0^*$, $[A]_{9,3} = 2v_0^*$, $[A]_{9,7} = \theta_x$, $\qquad$ $[A]_{9,9} = \theta_y$,

$[A]_{10,2} = 2u_0^*$, $[A]_{10,4} = 2v_0^*$, $[A]_{10,8} = \theta_x$, $\qquad$ $[A]_{10,10} = \theta_y$,

$[A]_{11,1} = u_{0,x}^*$, $[A]_{11,3} = v_{0,x}^*$, $[A]_{11,5} = -u_0^*/R_x$, $\qquad$ $[A]_{11,7} = \frac{1}{2}\theta_{x,x}$, $[A]_{11,9} = \frac{1}{2}\theta_{y,x}$,

$[A]_{12,2} = u_{0,y}^*$, $[A]_{12,4} = v_{0,y}^*$, $[A]_{12,6} = -v_0^*/R_y$, $\qquad$ $[A]_{12,8} = \frac{1}{2}\theta_{x,y}$, $[A]_{12,10} = \frac{1}{2}\theta_{y,y}$,

$[A]_{13,1} = u_{0,y}^*$, $\qquad$ $[A]_{13,2} = u_{0,x}^*$, $\qquad$ $[A]_{13,3} = v_{0,y}^*$, $[A]_{13,4} = v_{0,x}^*$,

$[A]_{13,5} = -v_0^*/R_y$, $\qquad$ $[A]_{13,6} = -u_0^*/R_x$, $\qquad$ $[A]_{13,7} = \theta_{x,y}$, $[A]_{13,9} = \theta_{y,y}$,

$[A]_{14,1} = 3\theta_x^*$, $[A]_{14,3} = 3\theta_y^*$, $[A]_{14,7} = 2u_0^*$, $[A]_{14,9} = 2v_0^*$, $[A]_{14,11} = \theta_x$, $[A]_{14,13} = \theta_y$,

$[A]_{15,2} = 3\theta_x^*$, $[A]_{15,4} = 3\theta_y^*$, $[A]_{15,8} = 2u_0^*$, $[A]_{15,10} = 2v_0^*$, $[A]_{15,12} = \theta_x$, $[A]_{15,14} = \theta_y$,

$[A]_{16,1} = \theta_{x,x}^*$, $\qquad$ $[A]_{16,3} = \theta_{y,x}^*$, $\qquad$ $[A]_{16,5} = -\theta_x^*/R_x$,

$[A]_{16,7} = u_{0,x}^*$, $\qquad$ $[A]_{16,9} = v_{0,x}^*$, $\qquad$ $[A]_{16,19} = u_0^*/R_x^2$,

$[A]_{17,2} = \theta_{x,y}{}^*,$ $\qquad [A]_{17,4} = 0,$ $\qquad [A]_{17,6} = -\theta_y{}^* / R_y,$

$[A]_{17,8} = u_{0,y}{}^*,$ $\qquad [A]_{17,10} = v_{0,y}{}^*,$ $\qquad [A]_{17,20} = v_0{}^* / R_y{}^2,$

$[A]_{18,1} = \theta_{x,y}{}^*,$ $\qquad [A]_{18,2} = \theta_{x,x}{}^*,$ $\qquad [A]_{18,3} = \theta_{y,y}{}^*,$ $\qquad [A]_{18,4} = \theta_{y,x}{}^*,$

$[A]_{18,5} = -\theta_y{}^* / R_y,$ $\qquad [A]_{18,6} = -\theta_x{}^* / R_x,$ $\qquad [A]_{18,7} = u_{0,y}{}^*,$ $\qquad [A]_{18,8} = u_{0,x}{}^*,$

$[A]_{18,9} = v_{0,y}{}^*,$ $\qquad [A]_{18,10} = v_{0,x}{}^*,$ $\qquad [A]_{18,19} = v_0{}^* / R_x R_y,$ $[A]_{18,20} = u_0{}^* / R_x R_y,$

$[A]_{19,7} = 3\theta_x{}^*,$ $[A]_{19,9} = 3\theta_y{}^*,$ $[A]_{19,11} = 2u_0{}^*,$ $[A]_{19,13} = 2v_0{}^*,$ $[A]_{19,15} = \theta_x,$ $[A]_{19,17} = \theta_y,$

$[A]_{20,8} = 3\theta_x{}^*,$ $[A]_{20,10} = 3\theta_y{}^*,$ $[A]_{20,12} = 2u_0{}^*,$ $[A]_{20,14} = 2v_0{}^*,$ $[A]_{20,16} = \theta_x,$ $[A]_{20,18} = \theta_y,$

$[A]_{21,7} = \theta_{x,x}{}^*,$ $\qquad [A]_{21,9} = \theta_{y,x}{}^*,$ $\qquad [A]_{21,11} = \tfrac{1}{2} u_{0,x}{}^*,$

$[A]_{21,13} = \tfrac{1}{2} v_{0,x}{}^*,$ $\qquad [A]_{21,19} = \theta_x{}^* / R_x{}^2,$ $\qquad [A]_{21,21} = \tfrac{1}{2} u_0{}^* \; R_x{}^2,$

$[A]_{22,8} = \theta_{x,y}{}^*,$ $\qquad [A]_{22,10} = \theta_{y,y}{}^*,$ $\qquad [A]_{22,12} = \tfrac{1}{2} u_{0,y}{}^*,$ $\qquad [A]_{22,14} = \tfrac{1}{2} v_{0,y}{}^*,$

$[A]_{22,20} = \theta_y{}^* / R_y{}^2,$ $\qquad [A]_{22,22} = \tfrac{1}{2} v_0{}^* \; R_y{}^2,$

$[A]_{23,7} = \theta_{x,y}{}^*,$ $[A]_{23,8} = \theta_{x,x}{}^*,$ $\qquad [A]_{23,9} = \theta_{y,y}{}^*,$ $\qquad [A]_{23,10} = \theta_{y,x}{}^*,$ $[A]_{23,11} = u_{0,y}{}^*,$

$[A]_{23,13} = v_{0,y}{}^*,$ $[A]_{23,19} = \theta_y{}^* / R_x R_y,$ $[A]_{23,20} = \theta_x{}^* / R_x R_y,$ $[A]_{23,21} = v_0{}^* / R_x R_y,$

$[A]_{24,11} = 3\theta_x{}^*,$ $[A]_{24,13} = 3\theta_y{}^*,$ $[A]_{24,15} = 2u_0{}^*,$ $\qquad [A]_{24,17} = 2v_0{}^*,$

$[A]_{25,12} = 3\theta_x{}^*,$ $[A]_{25,14} = 3\theta_y{}^*,$ $[A]_{25,16} = 2u_0{}^*,$ $\qquad [A]_{25,18} = 2v_0{}^*,$

$[A]_{26,11} = \theta_{x,x}{}^*,$ $[A]_{26,13} = \theta_{y,x}{}^*,$ $[A]_{26,21} = \theta_x{}^* / R_x{}^2,$

$[A]_{27,12} = \theta_{x,y}{}^*,$ $[A]_{27,14} = \theta_{y,y}{}^*,$ $[A]_{27,22} = \theta_y{}^* / R_y{}^2,$

$[A]_{28,11} = \theta_{x,y}{}^*,$ $[A]_{28,12} = \theta_{x,x}{}^*,$ $[A]_{28,13} = \theta_{y,y}{}^*,$ $[A]_{28,14} = \theta_{y,x}{}^*,$

$[A]_{28,21} = \theta_y{}^* / R_x R_y,$ $\quad [A]_{28,22} = \theta_x{}^* / R_x R_y,$

$[A]_{29,15} = 3\theta_x{}^*,$ $\qquad [A]_{29,17} = 3\theta_y{}^*,$ $\qquad [A]_{30,16} = 3\theta_x{}^*,$ $\qquad [A]_{30,18} = 3\theta_y{}^*,$

$[A]_{31,15} = \tfrac{1}{2} \theta_{x,x}{}^*,$ $\qquad [A]_{31,17} = \tfrac{1}{2} \theta_{y,x}{}^*,$ $\qquad [A]_{31,23} = \tfrac{1}{2} \theta_x{}^* / R_x{}^2,$

$[A]_{32,16} = \tfrac{1}{2} \theta_{x,y}{}^*,$ $\qquad [A]_{32,18} = \tfrac{1}{2} \theta_{y,y}{}^*,$ $\qquad [A]_{32,24} = \tfrac{1}{2} \theta_y{}^* / R_y{}^2,$

$[A]_{33,15} = \theta_{x,y}{}^*,$ $\qquad [A]_{33,17} = \theta_{y,y}{}^*,$ $\qquad [A]_{33,23} = \theta_y{}^* / R_x R_y.$ $\qquad$ A(3)

Individual terms of matrix [G]

$[G]_{1,1} = \partial / \partial x,$ $[G]_{1,3} = 1 / R_x,$ $[G]_{2,1} = \partial / \partial y,$ $[G]_{2,3} = 1 / R_{xy},$ $[G]_{3,2} = \partial / \partial x,$ $[G]_{3,3} = 2 / R_{xy},$

$[G]_{4,1} = 1 / R_{xy},$ $[G]_{4,2} = \partial / \partial y,$ $[G]_{4,3} = 1 / R_{xy},$ $[G]_{5,1} = -1 / R_x,$ $[G]_{5,3} = \partial / \partial x,$

$[G]_{6,2} = -1 / R_y,$ $[G]_{6,3} = \partial / \partial y,$ $[G]_{7,4} = \partial / \partial x,$ $[G]_{8,4} = \partial / \partial y,$ $[G]_{9,5} = \partial / \partial x,$

$[G]_{10,5} = \partial / \partial y,$ $[G]_{11,6} = \partial / \partial x,$ $[G]_{12,6} = \partial / \partial y,$ $[G]_{13,7} = \partial / \partial x,$ $[G]_{14,7} = \partial / \partial y,$

$[G]_{15,8} = \partial / \partial x,$ $[G]_{16,8} = \partial / \partial y,$ $[G]_{17,9} = \partial / \partial x,$ $[G]_{18,9} = \partial / \partial y,$ $[G]_{19,4} = 1,$

$[G]_{20,5} = 1,$ $\qquad [G]_{21,6} = 1,$ $\qquad [G]_{22,7} = 1,$ $\qquad [G]_{23,8} = 1,$ $\qquad [G]_{24,9} = 1.$ $\qquad$ A(4)